ISSN Print : 2621-3745
ISSN Online : 2621-3753
(Page.113-124)

Journal of Science and Applied Engineering (JSAE)
Vol. 5, No. 2, October 2022
DOI : 10.31328/jsae.v5i2.4074

DETERMINING IN-SITU FREQUENCY-INDEPENDENT ATTENUATION AND COMPLEX MODULUS OF PAVEMENT MATERIALS USING WAVELET POWER SPECTRAL DENSITY

***S. A. P. Rosyidi*[1,*]**

[1] *Department of Civil Engineering, Universitas Muhammadiyah Yogyakarta, Yogyakarta, Indonesia*
**Email: atmaja_sri@umy.ac.id*

Submitted : 30 September 2022; *Revision :* 25 October 2022; *Accepted :* 30 October 2022

ABSTRACT

Pavement vibration analysis can be used to determine the impact of damaging vibrations on the road and surrounding buildings or structures. Furthermore, this vibration can be utilized to calculate the dynamic properties of road pavement materials, such as the material's attenuation factor and damping ratio, as well as the complex modulus of the pavement material. However, estimating the degree of decrease in vibration amplitude at a given distance is challenging. Generally, vibration attenuation with length comprises two components: geometric damping and material damping. Geometric damping is related to the ground's qualities and the vibration's magnitude, while material damping is dependent on the nature of the source of the vibration. This study aims to determine the in-situ frequency-independent attenuation of pavement materials and then derive its corresponding material parameters, such as the damping ratio and the complex modulus of pavement layers. The wavelet power spectral density of vibration technique was used in this study to quantify the frequency-independent attenuation of geometric damping at various pavement structures in Malaysia and Indonesia. At each location, the energy from the seismic wave signal was calculated as a Morlet wavelet function of the signal amplitude. The vibration source's propagating waves were described by examining the recorded particle motions and significant energy components in the time-frequency domain. The complex modulus of pavement materials was then calculated using the values of material modulus and damping ratio obtained from the frequency-independent attenuation analysis. The results reveal that the wavelet power spectral density of the vibration method can adequately define the physical properties of the dynamic pavement material, such as attenuation frequency, damping ratio, and complex pavement modulus. This approach has the advantages of being quick, cost-effective, and non-destructive.

Keywords complex modulus; attenuation; pavement materials; wavelet power spectral density
Paper type Research paper

INTRODUCTION

In engineering issues involving dynamic loads at low to moderate strain levels, such as those caused by traffic, amplification during manufactured vibration and building activities, the natural vibration of earthquakes, and so on, frequency attenuation is an essential characteristic [1]. Radiation and material damping of layered material structures (such as pavements, embankment construction, soil profile, etc.) may be used to calculate the attenuation parameter of the material. During dynamic excitation, the energy of seismic waves is dissipated through several methods, including attenuation and the corresponding damping ratio in material dynamics [2]. These characteristics may be examined in situ using seismic techniques, which include measuring wave velocities as they propagate through soil material. Some vibration methods, such as spectral analysis of surface waves (SASW), impact resonant test (IR), and another dynamic testing, frequently employ material measurement methods. Both the theoretical and analytical foundations of this approach to soil examination are complete. The latest updates to the SASW technique were provided by Rosyidi [3].

The attenuation parameter has been studied through various in-field and in-lab experiments. Rix et al. [2] examined surface wave measurements to calculate the attenuation and damping ratio of a stratified soil deposit. The material shear damping ratio is calculated by inverting an attenuation curve

ISSN Print : 2621-3745
ISSN Online : 2621-3753
DOI : 10.31328/jsae.v5i2.4074
(Page.113-124)

built from the measured spatial attenuation of Rayleigh wave amplitudes. Surface wave analysis relies on seismic data; however, it is nonstationary, meaning its frequency content changes with time. Many scientists who study seismic observations rely on the Fourier transform as a primary tool for analysis. Any time-periodic function can be used in Fourier analysis if it can be expressed as the sum of sinusoids. It may be challenging to grasp the transformation results if Fourier analysis is used on random vibration signals under random settings. The study might lose some data about nonstationary seismic signals.

Furthermore, methods that allow temporal and frequency localization beyond standard Fourier analysis are required to retain time dependence and characterize the evolutionary spectrum properties of nonstationary systems. Wavelet analysis is increasingly used to examine localized fluctuations in power within a time series. The time-frequency spectrum is a breakdown of a time series that reveals the primary patterns of variability and how they change over time. Numerous investigations have used wavelet analysis in civil structures, such as in situ shear modulus [3], the phase velocity of soil structures [4], and soil damping ratio by using wavelet analysis [5].

The complex modulus of elasticity of bituminous mix is another crucial feature in pavement systems. A wide variety of standardized techniques exist for calculating this parameter. Some researchers have recently shown a strong desire for improved methods to study the mechanical characteristics of materials with complex moduli. Kweon and Kim [6] used an impact resonance test to calculate the asphalt concrete's complex modulus. Thirty-five HMA mixes were put through the IR and traditional dynamic modulus tests, all of which had different aggregate and binder properties. The reliability of the suggested method is demonstrated by comparing the dynamic modulus and phase angle determined using IR tests to those obtained using traditional dynamic modulus testing. However, only the upper half of the master curve of the dynamic moduli in the high-frequency level measured from the IR experiments at different temperatures was successfully obtained in Kweon and Kim's [6] study. It was observed that correct dynamic modulus master curves may be obtained by combining the IR test with the dynamic modulus test at 54.4 °C, or the IR test plus Witczak's prediction equation at 54.4 °C.

An alternative approach for characterizing the complex modulus of asphalt concrete was developed by Hasheminejad et al. [7] using an optical measuring technique (laser Doppler vibrometer). To find the complex modulus of asphalt concrete at its fundamental frequencies and to develop its master curve, they employed a frequency domain system identification approach based on analytical formulae (Timoshenko's beam theory). Compared to the master curve produced using the conventional four-point bending test, the technique's displayed master curve is very close to the master curve obtained using the conventional approach. The approach they've devised might one day replace the tried-and-true stiffness testing. However, a precise, complex modulus may be obtained using this approach at rather high frequencies.

The two-point bending complex modulus test with CRT-2PT trapezoidal beams is another technique for assessing the complex modulus of asphalt concrete [8]. The European Design Code [9] measured the complex modulus using a CRT-2PT two-point trapezoidal beam bending test equipment. As a result, CRT-2PT uses the strain control mode and a sine wave as its waveform. The 30 micro strain level, five test temperatures (5, 15, 20, 30, and 45 degrees Celsius), and six loading frequencies (1, 5, 10, 15, 20, and 25 Hz) were all employed in the tests. The trapezoidal beam specimen was vertically inserted and secured in the temperature control box at the start of the test, with a steady sine wave load applied to its top and reciprocated in its horizontal axis. Simultaneously, shear stress and bending moments were produced within the specimen. Their research found that converting between dynamic and complex modulus may be modeled with high accuracy. The suggested range for evaluating the dynamic modulus of high-modulus mixtures at varying evaluation temperatures was created based on the existing correlation model. However, the CRT-2PT two-point trapezoidal beam bending test protocol calls for asphalt concrete samples and is generally difficult to implement.

For assessing the in-situ attenuation factor and complex modulus of pavement materials, this research proposes a new method based on the mother wavelet of the Morlet for analyzing the wavelet power spectral density of vibrations. A field study's findings and applications at an actual pavement location are also highlighted.

Journal of Science and Applied Engineering (JSAE)
Vol. 5, No. 2, October 2022
DOI : 10.31328/jsae.v5i2.4074

METHOD

Location of Study

In this study, vibration data was collected using the surface seismic wave method on pavement locations on the UKM campus road in Malaysia, and several pavement sites in Indonesia. The flexible pavement structure at the test site comprises an asphalt concrete surface layer, a pavement aggregate base layer, and a soil subgrade layer.

Field Vibration Measurement

The surface wave approach is used in this study to acquire seismic vibration data. Figure 1 illustrates a seismic measurement configuration setup. A set of wave sources was used to generate and propagate surface seismic waves to gather the requisite vibration data. An impact source weighing 8–12 kg generates seismic waves at the low-frequency level, while small ball bearings are used at the high-frequency level. To produce vibrations on the pavement, the wave source is dropped freely at a predetermined height, causing vibration energy to propagate from the wave source's point to the sensor array, which is set in an imaginary line. Then, these waves are received using a combination of two accelerometers and geophones, depending on the receiver spacing. Thus, generated vibration signals are captured using a series of spectrum analysers for signal processing (Figure 1).

Several setups with receiver and source spacings of 5, 20, 80, and 160 cm were necessary to sample different depths of the pavement structure. The mid-point receiver spacing configuration was used in this measurement. In this setup, the shallow layers of the pavement profile were sampled with short receiver spacings and a high-frequency source, while the deeper layers were sampled with large receiver spacings and low-frequency sources.

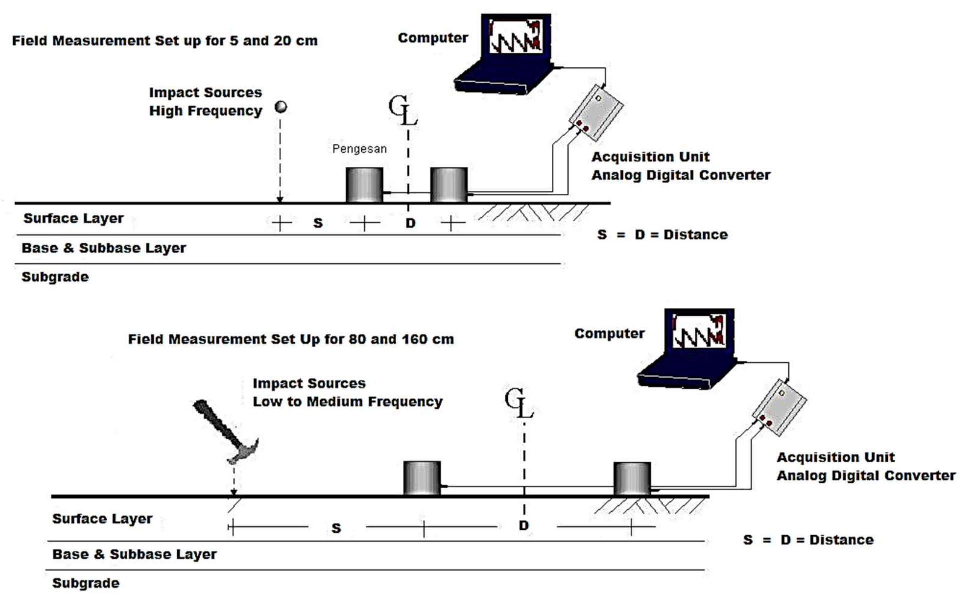

Figure 1. Vibration field configuration used on pavement measurement

Proposed Data Analysis

Theoretical Background of Wavelet Analysis

One definition of a wavelet states that it is a function of $\psi(t) \in L^2(\Re)$ that has a zero mean and is localized in time and frequency. The wavelet $\psi(t)$ can be dilated and translated to form a family of wavelets, which are as follows:

ISSN Print : 2621-3745
ISSN Online : 2621-3753
DOI : 10.31328/jsae.v5i2.4074
(Page.113-124)

$$\psi_{\sigma,\tau}(\tau) = \frac{1}{\sqrt{\sigma}}\psi\left(\frac{t-\tau}{\sigma}\right) \quad (1)$$

The parameter for the scale of the dilation is denoted by σ, whereas the value for the translation is denoted by τ where $\sigma, \tau \in \Re$ and $\sigma \neq 0$. The continuous wavelet transform, abbreviated CWT, is defined as the inner product of the family of wavelets denoted by $\Psi_{\sigma,\tau}(t)$ with the signal denoted by $f(t)$, which is expressed as follows:

$$F_w(\sigma,\tau) = \int_{-\infty}^{\infty} f(t)\frac{1}{\sqrt{\sigma}}\overline{\psi}\left(\frac{t-\tau}{\sigma}\right)dt \quad (2)$$

The time-scale map is denoted by $F_W(\sigma,\tau)$ while $\overline{\psi}$ is the complex conjugate of ψ. We can use the frequency domain to calculate the convolution integral in Equation 2. After the wavelet transform is performed, the function $f(t)$ can be reconstructed using Calderon's identity [10] in the mathematical expression of CWT:

$$f(t) = \frac{1}{C_\psi}\iint_{-\infty}^{\infty} F_W(\sigma,\tau)\psi\left(\frac{t-\tau}{\sigma}\right)\frac{d\sigma}{\sigma^2}\frac{d\tau}{\sqrt{\sigma}} \quad (3)$$

$$C_\psi = 2\pi\int\frac{\left|\widehat{\psi}(\omega)\right|^2}{\omega}d\omega < \infty \quad (4)$$

where $\widehat{\psi}(\omega)$is the frequency transform of the $\psi(t)$. There is an integrable discontinuity at $\omega = 0$ in the integrand in Equation 4, which means that $\int \psi(t)\,dt = 0$.

Construction of Wavelet Power Spectral Density

Here we define the total energy of a signal x(t) as the square root of its integrated magnitude.

$$E = \int_{-\infty}^{\infty}|x(t)|^2 dt \quad (5)$$

The energy density function, which is written in two dimensions, shows how much signal energy is at a given σ scale and τ location in CWT.

$$P_{F_w}(u,\xi) = |F_w(\sigma,\tau)|^2 \quad (6)$$

A scalogram is a plot of P_{Fw}, similar to a spectrogram, or the power spectrum density (PSD) generated by the short-time Fourier transform (STFT). In this study, STFT was replaced by wavelet transform. Integrating the scalogram over time, as shown below, lets us figure out how much energy the signal has.

$$P_{F_W} = \frac{1}{C_g}\int_{-\infty}^{\infty}\int_0^{\infty} P_{F_w}(\sigma,\tau)\frac{d\sigma}{\sigma^2}d\tau \quad (7)$$

where C_g is the wavelet function's admissibility constant $\psi(t)$.

Proposed Procedure of Attenuation and Complex Modulus Analysis

The suggested approach is shown below for attenuation analysis and complex modulus of pavement systems.

1. To determine the attenuation factor, the original signal $f(t)$ in the time domain was applied to wavelet spectrogram analysis. This signal was generated using the surface wave vibration method in field testing. The wavelet function and a set of scales are chosen to be used in the wavelet transform. The time and frequency resolution may be affected by the different wavelet functions. A Morlet wavelet function was employed as the mother wavelet in this study's CWT analysis. The Morlet wavelet, a Gaussian-windowed complex sinusoid, is a typical CWT wavelet. The following definitions apply to the time and frequency domains:

$$\Psi_0(t) = \pi^{-1/4}e^{imt}e^{-t^2/2} \quad (8)$$

ISSN Print : 2621-3745
ISSN Online : 2621-3753
(Page.113-124)

DOI : 10.31328/jsae.v5i2.4074

$$\hat{\psi}_0(s\omega) = \pi^{-1/4} H(\omega) e^{-\frac{(s\omega-m)^2}{2}} \quad (9)$$

where m denotes the wave number and H denotes the Heaviside function. Figure 2 shows the Morlet wavelet's time and frequency domain plot. The Morlet wavelet is presented in Figure 2 within an adjustable parameter m of 7, which is employed in this investigation. This characteristic can be utilized at low frequencies to reproduce seismic surface wave signals correctly. The time resolution plot's Gaussian second-order exponential decay generates the best time localization

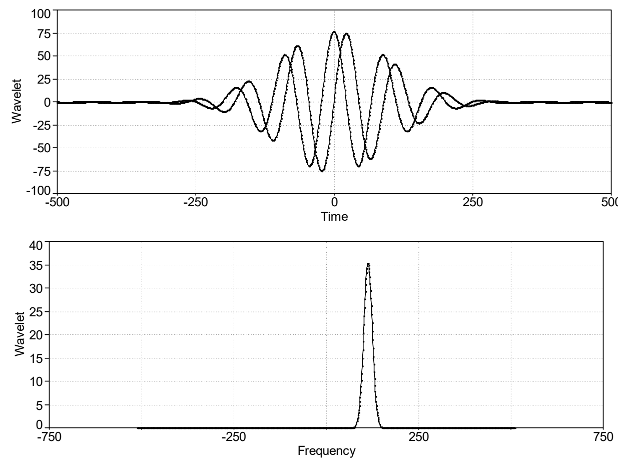

Figure 2. Time domain of real and imaginary parts and its transformation in the frequency domain of Morlet wavelet.

2. The wavelet scalogram is created by conducting the wavelet transform (Equation 2) and combining the seismic trace's calculated convolution with a scaled wavelet definition. From Torrence and Compo [11] study's, the wavelet scale may be computed as the fractional power of two using the given equations:

$$s_j = s_0 2^{j\delta_j}, j = 0, 1, \ldots, J \quad (10)$$

$$J = \delta j^{-1} \log_2\left(\frac{N\delta_t}{s_0}\right) \quad (11)$$

where s_0 is the lowest resolvable scale = $2\delta_t$, δ_t is the interval spacing, and J is the highest scale.

3. The signal's scale-dependent wavelet energy spectrum (scalogram) is converted into a frequency-dependent wavelet energy spectrogram for direct comparison with the Fourier energy spectrum. The time and frequency localization thresholds are used to achieve the CWT filtering on the wavelet spectrogram. The CWT filtration is established in this work based on the basis of a simple truncation filter idea that just concerns a passband and a stopband. The filter values between the passband and the stopband are then determined by setting threshold values in the time and frequency domains. Straight filtering is possible in all three dimensions of time, frequencies, and spectral energy. The noisy or irrelevant signals may be removed by zeroing the spectrum energy. As a result, they are eliminated while reconstructing the time domain signal. Thus, the desired spectrum of the signals is passed while the spectrum energy remains constant. Rosyidi [3] introduced a CWT filtering design.
4. The time series of a seismic trace is reconstructed using Equation 3, and the Wavelet PSD or spectrogram is derived from cleaned-up signals.
5. The Wavelet PSD ratio is calculated by plotting the experimental power spectrum ratio vs frequency against the experimental power spectrum ratio.
6. The following equation [5] may be used to calculate how the Wavelet PSD to frequency ratio evolves over time:

Journal of Science and Applied Engineering (JSAE)
Vol. 5, No. 2, October 2022
ISSN Print : 2621-3745
ISSN Online : 2621-3753
DOI : 10.31328/jsae.v5i2.4074
(Page.113-124)

$$ln\left[\frac{W_f^{R_2}(\sigma,\tau)}{W_f^{R_1}(\sigma,\tau)}\right] = ln\left\{\left(\frac{R_1}{R_2}\right)^n \cdot G(R) \cdot G(I) \cdot K(R)\right\} - \alpha(f)(R_1 - R_2) \qquad (12)$$

$$ln\left[\frac{W_f^{R_2}(\sigma,\tau)}{W_f^{R_1}(\sigma,\tau)}\right] = k - \alpha(f)(\Delta R) \qquad (13)$$

7. Suppose two receivers (geophones or accelerometers) are employed. In that case, the distances between them are R_1 and R_2, the geometric spreading factor is $G(R)$, the instrumentation correction factor is $G(I)$, the refracted and transmitted wave correction factor is $K(R)$. The frequency-independent attenuation factor is $\alpha(f)$.
8. The attenuation factor of soil structures can be determined by comparing theoretical and experimental regression. The attenuation factor for each wavelength can be calculated without having to do a continuation of the previous procedures. Another procedure for determining the frequency-independent and dependent attenuation coefficients of pavement materials is as follows [12]:

$$\alpha_0 = \frac{\alpha}{f} = \frac{2\pi\xi}{V_R} \qquad (14)$$

$$\alpha = \frac{2\pi f\xi}{V_R} \qquad (15)$$

where α_0 is the material frequency-independent attenuation coefficient (m^{-1}) and ξ is the damping ratio of materials.

9. The complex shear modulus (G^*) can be calculated using Gucunski's [13] equation, which requires the damping ratio (ξ) and shear modulus (G):

$$G^* = G(1 + 2\xi) \qquad (16)$$

$$G = \rho \times V_S{}^2 \qquad (17)$$

In these equations, V_S is the velocity of the shear wave, g is the acceleration of the gravitational field, μ is Poisson's ratio of the material, and ρ is the mass density of the material. Nazarian and Stokoe [14] determined that the modulus of the material achieves its maximum value when the strain is less than 0.001%. The shear modulus of a material is considered constant within this strain range. Kweon and Kim [6] proposed the following relationship between the shear modulus (G), the phase angle (ϕ), and the elastic modulus (E) in order to determine the complex elastic modulus (E^*):

$$E^* = \frac{E}{cos(\phi)} \qquad (18)$$

$$E = 2G(1 + 2\mu) \qquad (19)$$

$$\phi = tan^{-1}(2\xi) \qquad (20)$$

Kweon and Kim [6] indicated that the damping ratio (ξ) for asphalt concrete materials in the impact resonant testing frequency spectrum ranged from 1% to 10%. It is also highly dependent on the frequency and temperature of loading.

DISCUSSION

Wavelet Power Spectrum Density of Pavement's Seismic Data

Figure 3 shows signal data in the time domain produced from this experiment. Measurement signals indicate that seismic transient impulses can be recorded clearly. Coherent noise is leading cases by the surface refraction and reflection of body waves in the case of road pavement (reflected refraction waves). In contrast, time-domain signal recordings cannot detect and measure coherent noise from these body waves.

Journal of Science and Applied Engineering (JSAE)
Vol. 5, No. 2, October 2022
DOI : 10.31328/jsae.v5i2.4074

The time-recorded seismic waves were subsequently subjected to time-frequency (TF) analysis. Figure 4 displays the resolution analysis results of the TF evaluation using the Morlet basis and derivative levels ranging from 12 to 25. According to the four results of the TF, the seismic signal is detectable on the complete signal recording. On the 5 cm sensor distance spectrogram, surface waves are identified between 4 and 8 kHz, but body waves are identified at higher frequencies (above 10 kHz). After both sensors detect body wave propagation, surface waves are recorded. Because of the nearness of the sensor, both body and surface waves are captured nearly simultaneously. Nevertheless, surface wave energy predominates over body wave energy. In vibration analysis, the effect of body waves on the recordings is defined as the near field effect. In this circumstance, the perturbation of body wave energy is also considered when computing the phase velocity of surface waves. Also, neither sensor can detect the coherent noise of body wave reflection at 5 cm.

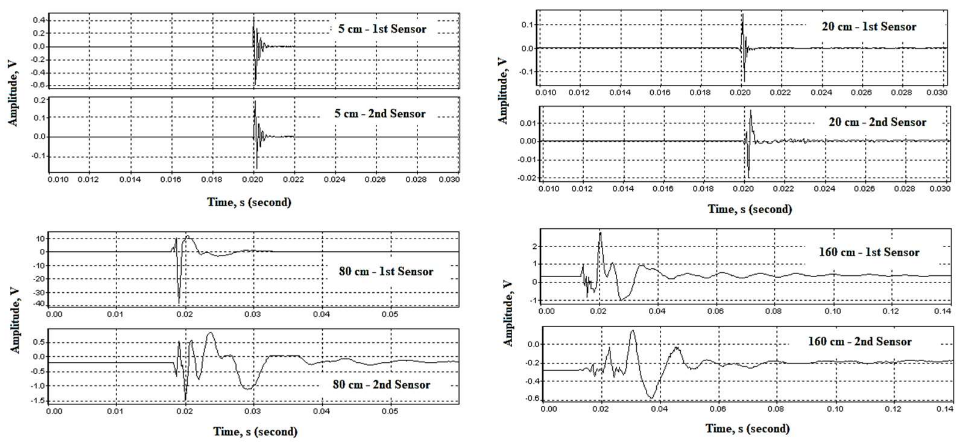

Figure 3. Waveforms of seismic surface waves observed by two receivers

To reconstruct the necessary signals from the recordings, a filtering analysis is performed, and CWT's time-frequency (TF) analysis is employed to solve the issue of recognizing the spectrum pattern of nonstationary seismic wave signals. The time-frequency threshold-based filtration method proposed by Rosyidi [3] is implemented. The method can identify and remove the spectrum of noise from recorded data. The clarity of response spectrum analysis can be improved through denoising and signal cleaning. There are two primary techniques to determining thresholds in wavelet filtering. Determining a signal's time-frequency domain is the first step towards isolating and reconstructing its core components. The time and frequency domains limit the ability to filter a spectrogram. In this study, the noise signal frequency range is defined as the wavelet filtering threshold, suggesting that only seismic wave signals of relevance remain in the spectrogram after the noise signals have been filtered away. Using the inverse wavelet transform, denoised seismic signals are then created as the final step in the wavelet filtering approach. Figure 5 also indicates energy reduction in both spectra. These energy losses can be utilized to calculate a material's attenuation factor.

Attenuation and Damping Ratio Analysis of Pavement Structures

Figure 5 shows an indication of the experimental energy losses data at 160 cm receiver of the wavelet PSD between both signals from the logarithmic natural function of the spectrogram (Wf_2) over the first signal magnitude (Wf_1) vs frequency. The ratio demonstrates the frequency dependency decay factor curve from R-wave motion vibration data (Figure 5). The decay factor curve experimental data is then subjected to a basic linear regression analysis. The experimental regression equation is written as:

$$ln\left[\frac{W_f^{R_2}(u,s)}{W_f^{R_1}(u,s)}\right] = -0.0031(f) + 1.1471 \qquad (21)$$

ISSN Print : 2621-3745
ISSN Online : 2621-3753
DOI : 10.31328/jsae.v5i2.4074
(Page.113-124)

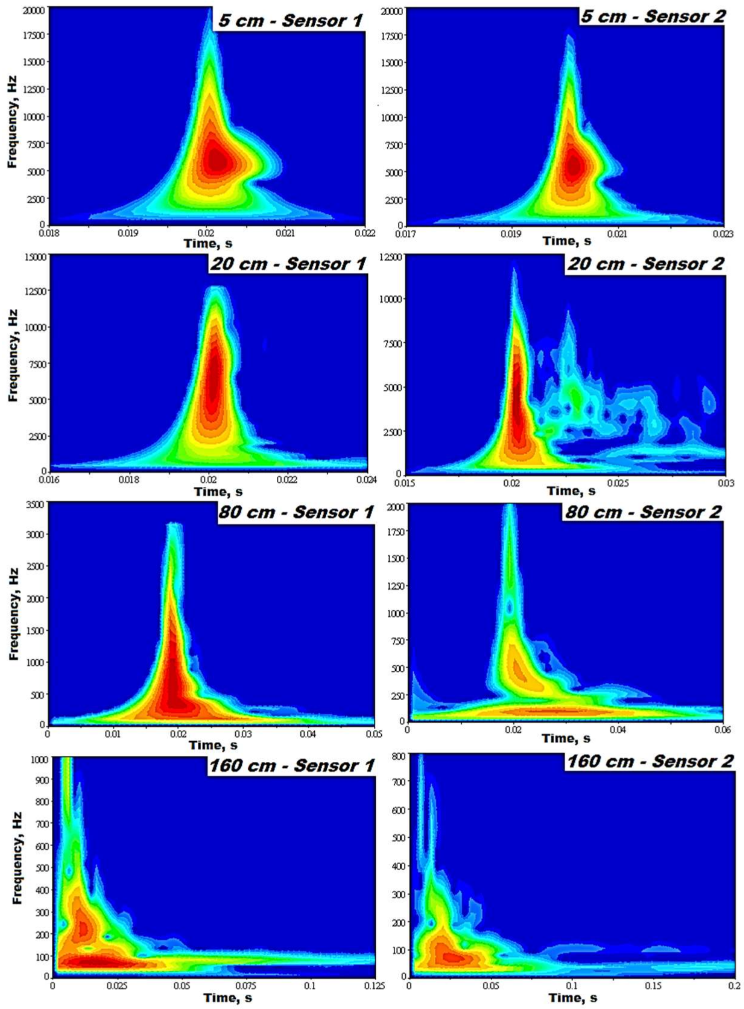

Figure 4. Wavelet PSD results from seismic surface waves observed by two receivers

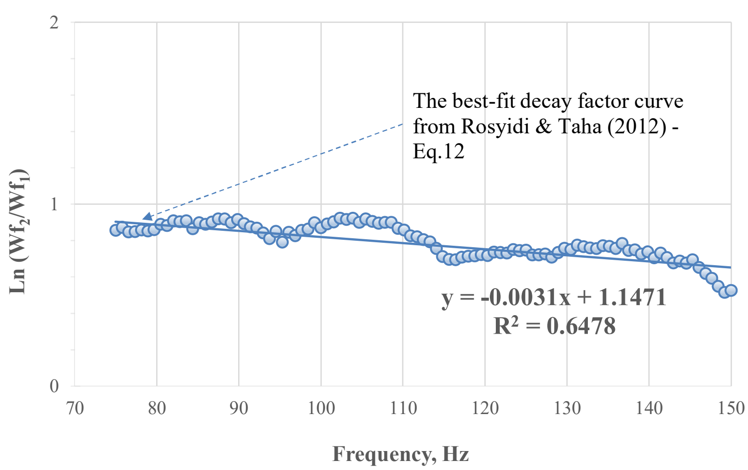

Figure 5. Experimental data plotting of the wavelet PSD of energy losses from 160 cm receiver spacing configuration and its best-fit decay factor curve

The theoretical regression analysis of attenuation derived can then be written as:

$$ln\left[\frac{W_f^{R_2}(u,s)}{W_f^{R_1}(u,s)}\right] = -\alpha(f)(\Delta R) + k$$

$$= -1.6\alpha(f) + k \qquad (22)$$

At a frequency range of 75-150 Hz, the best-fit value of the frequency-independent attenuation coefficient of the pavement layer in a 160 cm vibration measurement configuration is computed as 1.938×10^{-3} s/m. The observed layer at 160 cm receiver spacing is the pavement subgrade layer based on the measurement configuration, attenuation coefficient value, and average shear wave velocity. Table 1 summarizes the frequency range of each layer of the pavement structure as well as the findings of frequency-independent attenuation. According to the results, the asphaltic layer has a lower average attenuation value than the base and subgrade layers. They also show that material stiffness decreases while attenuation increases with depth.

TABLE I. THE INTERESTED FREQUENCY RANGE OF EACH LAYER AND THE RESULT OF FREQUENCY-INDEPENDENT ATTENUATION

Material of Pavement Layer	Interested frequency range (Hz) from Wavelet PSD Analysis	α_0 ($\times 10^{-3}$ s/m) – Frequency-Independent Attenuation Coefficient
Surface Layer: Asphalt	8 – 15k	0.427 – 1.233 (Average 0.886)
Foundations: Base and Subbase	750 – 2k	1.077 – 3.213 (Average 1.819)
Soil Subgrade	50 - 200	4.118 – 7.354 (Average 4.836)

As shown in Figure 6, the values of the frequency-independent attenuation coefficient and the average shear wave velocity found in this study were compared with experimental results acquired by other researchers such as Yang [15], Woods [16], and Athanasopoulos et al. [12]. Woods and Jedele's study [17] also defined soil categories based on frequency-dependent vibration attenuation at 5 Hz.

From Table 1 and Figure 6's plot of the attenuation coefficient of asphalt pavement materials with depth show that the values obtained in this study was found from 0.427 to 1.233×10^{-3} s/m are identical the values reported by Yang [15] for the rock class attenuation coefficient ($0.385 - 0.775 \times 10^{-3}$ s/m). Woods [16] measured the material attenuation from a 5 Hz generated vibration and found it to be less than 0.3×10^{-3} m^{-1} as a function of frequency. Moreover, by dividing the value of the frequency-dependent attenuation coefficient by the frequency of vibration (5 Hz), the amplitude of the rock's frequency-independent attenuation coefficient was determined to be fewer than 6×10^{-5} s/m [16]. As a result, asphaltic materials have a higher attenuation value than rock materials. This is due to the decreased rigidity of asphaltic materials compared to rocks.

In this investigation, the average attenuation of the base and subbase, and subgrade layer material are 1.819×10^{-3} s/m with values ranging from 1.077 to 3.213×10^{-3} s/m and 4.836×10^{-3} s/m in ranging from 4.118 to 7.354×10^{-3} s/m. According to Woods and Jedele [17], the attenuation factor of the pavement subgrade layer in this investigation falls into Class 1 (soil). In general, the results match well with those of Anthanasopoulos et al. [12], who determined the range of soil attenuation coefficients. This study's attenuation coefficient is still within the upper and lower bounds of the values obtained by [12]:

$$\alpha_0 = 3.17 \times 10^{-3} \times e^{-\frac{Vs}{500}} \text{ (best fit)} \qquad (23)$$

$$\alpha_0 = 1.15 \times 10^{-3} \times e^{-\frac{Vs}{500}} \text{ (lower bound)} \qquad (24)$$

Journal of Science and Applied Engineering (JSAE)
Vol. 5, No. 2, October 2022
ISSN Print : 2621-3745
ISSN Online : 2621-3753
DOI : 10.31328/jsae.v5i2.4074
(Page.113-124)

In comparison to Yang's [15] research, Figure 6 demonstrates that the attenuation factor of this study is close to the top bound of Yang's [15] attenuation coefficient range for unsaturated loose sand materials, which is most probably related to material variances.

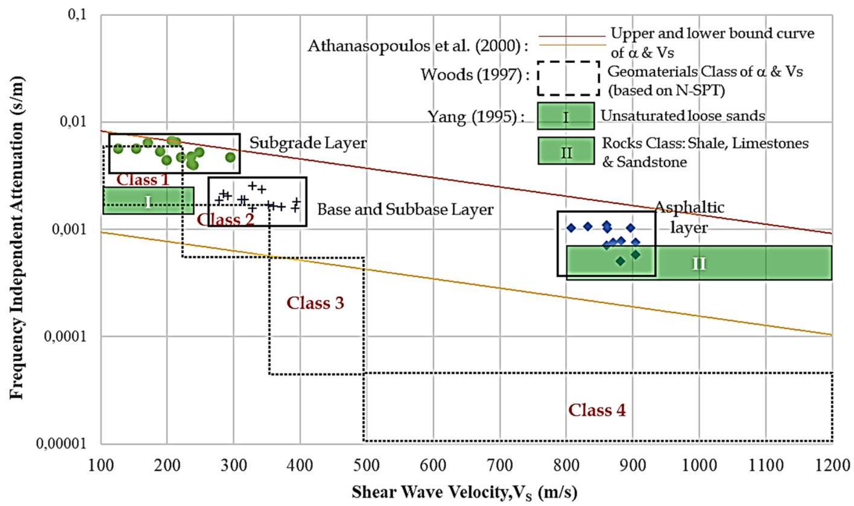

Figure 6. Comparison of frequency-independent attenuation coefficient versus shear wave velocity of pavement layers from this study to the results of various studies.

Complex Elastic Modulus of Pavement Structures

After the attenuation coefficient has been obtained, the damping ratio of the pavement materials can be determined. The shear modulus was calculated using Equation 17, and the shear wave velocity was found by inverting the R-wave velocity dispersion curve obtained from a surface wave measurement (Figure 7). Thus, by using the measured parameter of shear modulus and the damping ratio, the complex shear modulus may be derived. An example of the shear wave velocity profile is presented in Figure 7. The shear wave velocity significantly decreases with depth, as seen by the stiffness profile of the pavement structure. At several pavement sites, the average shear wave velocity of the asphaltic layer was found to be 840 m/s, whereas that of the base and subgrade layers was 297 and 146 m/s, respectively.

The shear and complex shear moduli of the pavement profile and the damping ratio, are shown in Figure 7. When compared to other studies, the damping ratio of the pavement structure used in this one has the lowest value. The asphaltic layer has a damping ratio of 0.62 percent, the base has a damping ratio of 1.31 percent, and the subgrade has a damping ratio of 1.92 percent. The results for the shear and complex shear moduli are very similar. Both the moduli of the asphaltic layer are more than 1,600 MPa, with the higher value being more typical. Whereas the shear and complex shear moduli of the soil subgrade layer are 41 and 42 MPa, those of the base layer modulus are 186 and 191 MPa, respectively.

The complex shear modulus of the asphalt layer (1,643 MPa) measured in this study (Figure 7) yields a larger dynamic modulus value than that determined by Christensen [18], who determined the complex shear modulus of the asphaltic mixture (881 MPa) using the Field Shear Test (FST). This could be because of the unique properties of asphalt's viscosity and the 10 Hz frequency and 40 °C temperature used in Christensen's experiment.

This investigation determined the complex elastic modulus to be 10.924 GPa (Figure 8), which is somewhat less than the range of complex elastic moduli obtained by Kweon and Kim's IR technique [6]. It is because to the differing asphalt material qualities, temperatures, and lower frequency of set up employed in both samples. Finally, the results reveal that Wavelet PSD can accurately define the dynamic stiffness of the pavement layer in terms of attenuation coefficient, damping ratio, and complex shear and elastic modulus for pavement design and evaluation.

ISSN Print : 2621-3745
ISSN Online : 2621-3753
(Page.113-124)

DOI : 10.31328/jsae.v5i2.4074

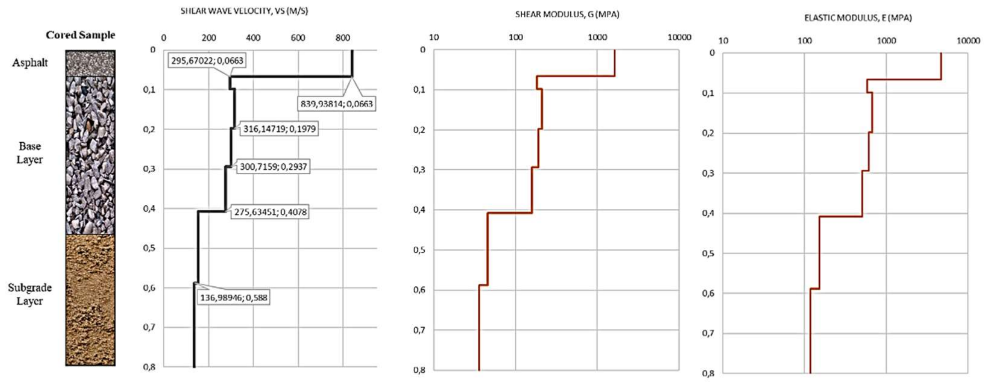

Figure 7. Shear wave velocity, shear and elastic modulus profile from the inversion of surface wave (vibration) measurement

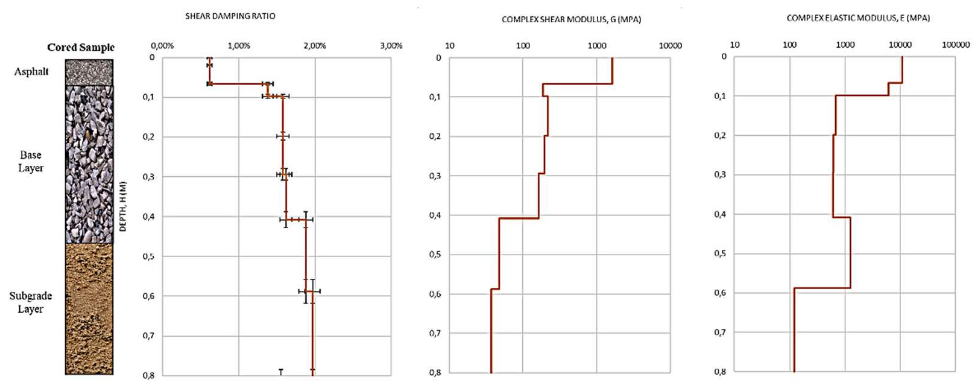

Figure 8. Shear damping ratio, complex shear modulus and elastic modulus profile from this study

CONCLUSION

This study proposed the Wavelet PSD approach as a method for in-situ measurement and calculation of attenuation analysis, damping ratio, and complex modulus of pavement materials. The attenuation factors found in this study and those reported in other investigations were not significantly different. The frequency-independent attenuation coefficient of asphalt layer was found to be 0.427 to 1.233 $\times 10^{-3}$ s/m with an average value of 0.886 $\times 10^{-3}$ s/m, while the frequency-independent attenuation coefficients of foundation layers, i.e., base and subbase materials, and soil subgrade layer were found to be 1.077 - 3.213 $\times 10^{-3}$ s/m (average = 1.819 $\times 10^{-3}$ s/m) and 4.118 - – 7.354 $\times 10^{-3}$ s/m (average = 4.836 $\times 10^{-3}$ s/m), respectively. The complex shear modulus of the asphalt layer produced in this study was 1,643 MPa, which is a higher dynamic modulus value than that reported in prior studies using Field Shear Testing procedures. This is because of the different viscosities of asphalt and the way testing is set up for frequency and temperature. In this study, the complex elastic modulus of asphalt pavement material was calculated using the material damping ratio, which was determined using the attenuation factor, and other parameters such as the Poisson ratio and shear modulus of asphalt material. The complex elastic modulus measured in this study was 10.924 GPa, which is less than the range of complex elastic moduli obtained using the Impact Resonance Test method. This is because the asphalt utilized in each sample had varying quality, temperatures, and usage frequencies. Thus, the Wavelet PSD approach may be used to characterize the physical attributes of the dynamic stiffness of pavement materials in terms of attenuation coefficient, damping ratio, and complex modulus. This method is advantageous because it is quick, enables testing in situ, is cost-effective, and does not cause significant damage to the pavement structures.

ACKNOWLEDGMENT

This study was made possible thanks to funding from the Program Hibah Penelitian Internal at Universitas Muhammadiyah Yogyakarta 2020–2021. The author wishes to convey their appreciation to those responsible for sponsoring this research.

REFERENCES

[1] Vucetic, M. & Dobry, R. 1991. Effect of Soil Plasticity on Cyclic Response. *Journal of Geotechnical Engineering* 117(1): 89-107.

[2] Rix, G.J., Lai, C.G. & Spang, A.W., Jr. 2000. In Situ Measurement Of Damping Ratio Using Surface Waves. *Journal of Geotechnical and Geoenvironmental Engineering* 126(5): 472 – 480.

[3] Rosyidi, S.A.P. 2009. Wavelet Analysis of Surface Wave for Evaluation of Soil Dynamic Properties, Ph.D. Thesis, the National Universiti of Malaysia, Bangi.

[4] Kim, D-S & Park, H-C. 2002. Determination of Dispersive Phase Velocities for SASW Method Using Harmonic Wavelet Transform. *Soil Dynamics and Earthquake Engineering* 22: 675–684.

[5] Rosyidi, S.A.P. & Taha, M.R. 2012. Wavelet Spectrogram Analysis of Surface Waves Technique for Dynamic Soil Properties Measurementon Soft marine Clay Site. *In Seismic Waves, Research and Analysis* (Ed. Masaki Kanao). Intech, Rijeka, Croatia.

[6] G. Kweon and Y.R. Kim, "Determination of Ashpalt Concrete Complex Modulus with Impact Resonance Test, " Transportation Research Record: *Journal of the Transportation Research Board*, No.1970, pp.151-160, 2006.

[7] N. Hasheminejad, C.Vuye, A. Margaritis, W. Van den bergh, J. Dirckx, and S. Vanlanduit, "Characterizing the Complex Modulus of Asphalt Concrete Using a Scanning Laser Doppler Vibrometer" *Materials* 12, No. 21: 3542, October 2019. https://doi.org/10.3390/ma12213542.

[8] L. Guo, Q. Xu, G. Zeng, W. Wu, M. Zhou, X. Yan, X. Zhang, and J. Wei, "Comparative Study on Complex Modulus and Dynamic Modulus of High-Modulus Asphalt Mixture," *Coatings* 11, No. 12: 1502, December 2021. https://doi.org/10.3390/coatings11121502

[9] J.-F. Corté and J., -P. Serfass, "The French Approach to Asphalt Mixtures Design: A Performance-Related System of Specifications," *Assoc.Asph. Paving Technol*., 69, pp.794–834, 2000.

[10] I. Daubechies, *Ten Lecturers on Wavelets. Society for Industrial and Applied Mathematics*, University City Science Center Philadelphia, PA USA, 1992, 369p.

[11] C. Torrence and G.P. Compo, "A Practical Guide To Wavelet Analysis, " *Bull. of the Amer. Meteor. Soc.,*Vol.79(1), 1998, pp.61-78.

[12] G.A. Athanasopoulos, P.C. Pelekis, and G.A. Anagnostopoulos, "Effect of Soil Stiffness in the Attenuation of Rayleigh-wave Motions From Field Measurements," *Soil Dynamic and Earthquake Engineering*, Vol.19, 2000, pp.277-288.

[13] N. Gucunski, Generation of Low Frequency R-Waves for The Spectral-Analysis-of-Surface-Waves Method, *PhD dissertation*, Michigan: The University of Michigan, 1991.

[14] S. Nazarian, S. & K.H. II Stokoe, In situ Determination Of Elastic Moduli Of Pavement Systems By Spectral-Analysis-Of-Surface-Wave Method (Theoretical Aspects), *Research Report 437-2. Center of Transportation Research, Bureau of Engineering Research*, The University of Texas at Austin, 1986.

[15] X.J. Yang, "Evaluation of Man-Made Ground Vibration, " *Proc. 3rd Int. Conf. on Recent Advances in Geotechnical Conference Earthquake Engineering and Soil Dynamics 3*, St. Louis (USA), 1995, pp.1345-1348.

[16] R.D. Woods, *Dynamic Effects of Pile Installations on Adjacent Structures*, NCHRP Synthesis 253, National Research Council, Transportation Research Board, National Cooperative Highway Research Program, 1997.

[17] R.D. Woods and L.P. Jendele, "Energy-Attenuation Relationships from Construction Vibrations," In G. Ga-zetas & E.T. Selig (ed.), *Vibration Problems in Geotechnical Engineering*, Special Publication ASCE, New York, 1985, pp. 229-246.

[18] D.W. Christensen Jr., Sensitivity Evaluation Of Field Shear Test Using Improved Protocol And Indirect Tension Strength Test, *Contractor's Final Report*, National Cooperative Highway Research Program Transportation Research Board of the National Academic, Web Document 56, Project 9-18(1), 2003.